Synthesis and Determination of Molar Absorptivity of 3-Monolayer CdSe Nanoplatelets

Madalyn Hymowitz

Department of Chemistry, SUNY Geneseo
May 8, 2024
Honors Thesis, under the supervision of Dr. Jeffrey Peterson

Novel-sized CdSe nanoplatelets (NPLs) were synthesized, their optical properties characterized, and their lateral size was determined by multiple methods. CdSe NPLs were found to be 3-monolayers (MLs) thick by UV-Vis absorption, fluorescence spectroscopy, and in comparison to literature values. Transmission electron microscopy (TEM) was used to determine the lateral size of the NPLs. Dynamic light scattering (DLS) was also investigated as a potential new method to measure lateral growth; however, lateral sizes from DLS were about two orders of magnitude larger than those determined by TEM, so DLS proved to be an invalid replacement for TEM at this time. Inductively coupled plasma-optical emission spectroscopy (ICP-OES) was used to determine the molar absorptivity values of the NPLs, which ranged from approximately 1.2 to 3.5 $\times$ 10^{8} $M^{-1}cm^{-1}$ depending on the lateral size. These values are consistent with those reported in literature for 4- and 5- ML NPLs and extend critical NPL characteristics to previously undescribed NPLs.

Introduction

Nanoparticles (NPs) have been widely investigated and have been shown to have a variety of uses in many fields, including medicine and electronics.[1,2] For example, due to their small size NPs are able to easily penetrate the cell wall and blood-brain barrier to deliver drugs and other therapeutic agents to cancer cells.[3] They can be used for detection, location, and characterization of cancer.[3,4] Their small size also allows for them to be covalently linked with biorecognition molecules.[5] Additional applications have been seen for photovoltaics,[6] light emitting diodes,[7] lasers,[8] and biological imagings.[9] In terms of electronics, NPs are of interest because they can be used to produce materials on the nanoscale that exhibit unique and beneficial physiochemical properties. For example, it is well known that their emission peaks and optical properties depend strongly on the size of the NP used.[4,10] In addition, the *shape* of the NP can also dramatically alter its physiochemical properties.

Nanoparticles can be generally classified into three different shapes: zero-dimensional quantum dots (QDs), one-dimensional nanorods (NRs) and two-dimensional nanoplatelets (NPLs (Figure 1). What differentiates these three types of NPs are the physical dimensions in which electron-hole pairs (excitons) are confined by the nanostructure. In spherical QDs, excitons are confined in all three dimensions by the QD surface (effectively a 3D particle in a box) and are thus referred to as 0D structures. In cylindrical NRs, excitons are confined in two dimensions along the NR waist, but free along the length of the rod, thus referred to as a 1D particle. NPLs are confined in only one dimension (effectively a 1D particle in a box), but free in two dimensions.

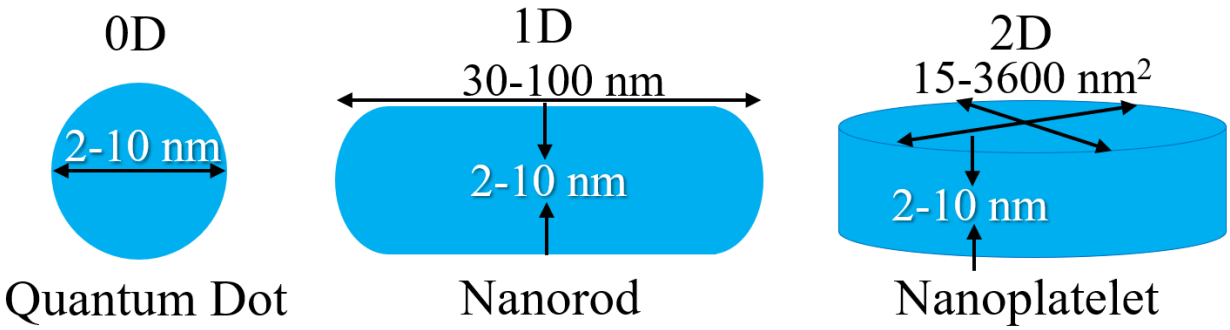

Figure 1. Cartoon representation of three possible configurations of nanoplatelets with relative sizes.

The aforementioned freedom to grow laterally gives NPLs interesting optical properties compared to other shapes. For example, in an absorption spectrum the absorption peak wavelength (x-axis) is uniquely determined by the NPL thickness; however the molar absorptivity is proportional to the NP volume thus the absorbance values (y-axis) can be tuned to almost arbitrarily large values by increasing the NPL lateral size. This study focused on CdSe NPLs in particular. Compared to other nanoparticles CdSe are relatively new, first discovered in 2006 in their wurtzite structure,[11] then in 2008 in their zincblende structure.[12] The molar absorptivity values of 4- and 5-ML CdSe NPLs were found to be on the order of 10^7-10^8 $M^{-1}cm^{-1}$

respectively with the specific values being dependent on the lateral size.[13] Compared even to CdSe QDs whose molar absorptivity is on the order of 10^5 $M^{-1}cm^{-1}$, these values are larger by 10^2 and 10^3.[14,15] Due to these extremely large molar absorptivities, NPLs have generated significant interest for optoelectronic applications, such as LEDs, photo and laser diodes, sensors, solar cells, photocatalysts and more.[13]

Previous work has been done growing NPLs of varying thicknesses and lateral sizes, and characterizing their optical properties.[13,16,17] The absorption peak is uniquely determined by the NPL thickness (because the exciton is strongly confined in the z-dimension[16]) and not the lateral size; thus there is also a special relationship between absorption peak and the number of NPL MLs. As shown in figure 2A, in a 4-ML CdSe NPL the first absorption peak (of the characteristic double peaks) occurs at 517 nm and is constant regardless of lateral size. However, the same is not true for other NP shapes, nor if the thickness of the NPL changes. In 0D QDs (Figure 2B), it is apparent that the wavelength of maximum absorbance changes with lateral size. This is also true when NPLs of different thicknesses (3-, 4-, and 5-MLs) are plotted against each other (Figure 2C). For fluorescence, a trend similar to that seen in absorbance occurs, although its peak involves a bathochromic (red) shift in relation to the first peak of the double peaks in its absorbance spectrum (green curve in Figure 2A).

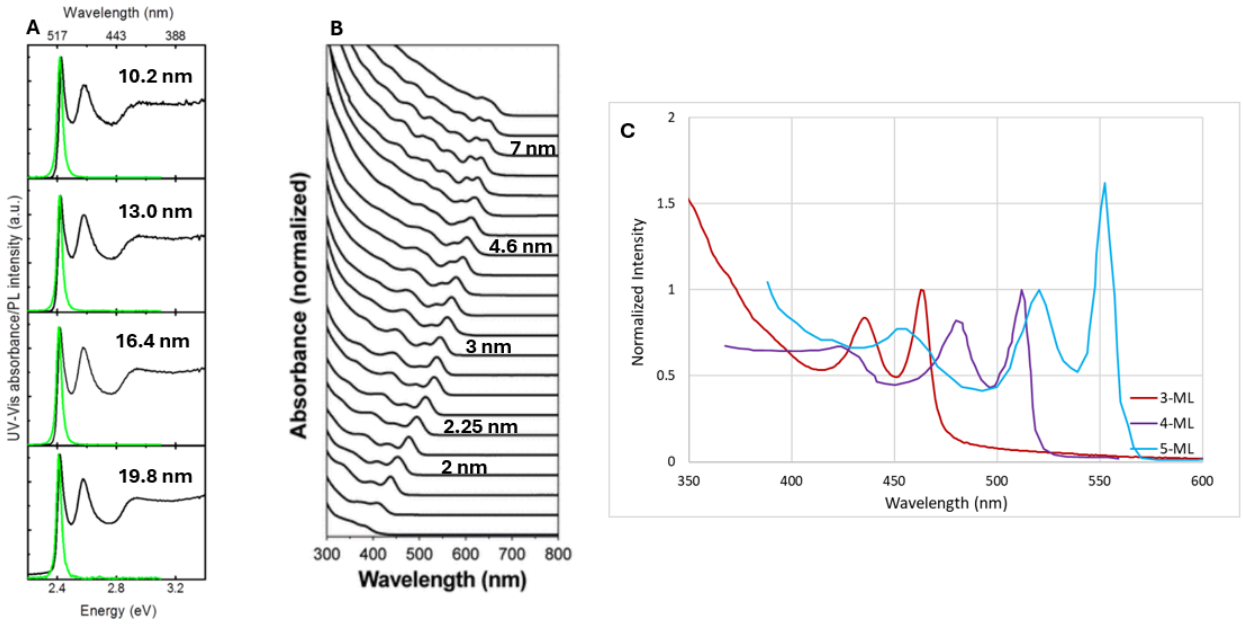

Figure 2. Example of a characteristic absorbance and fluorescence spectra for **A)** 4-ML CdSe NPLs at different lateral sizes[13] compared to that of **B)** normalized absorbance spectra of quantum dots at different lateral sizes[15] and **C)** normalized absorbance spectra for CdSe NPLs at different thicknesses using current work for 3-ML NPLs and data extrapolated from literature values for 4- and 5-ML NPLs.[13]

In previous works, measurements of lateral growth of CdSe NPLs have been obtained using transmission electron microscopy (TEM).[13] This geometric information enables one to calculate the number of Cd and Se atoms per NPL based on material properties such as the lattice constants and density. After digesting NPL solutions of known absorbance in acid and measuring Cd and Se concentrations using inductively coupled plasma - optical emission spectrometry (ICP-OES), the absorption cross-section and the molar absorptivity can be calculated. These values are ultimately related to the NPLs lateral sizes and thickness.[13] While TEM has been shown to be an effective and accurate method of measuring lateral growth, its analysis is time consuming. Dynamic light scattering (DLS) can be done in minutes without the additional by-hand analysis that TEM requires and could be a possible alternative method to measure lateral size. Previous studies have shown DLS as a method of measuring nanoparticles, especially QDs, with sizes ranging from 1 nm-1 μm.[18] DLS is fast, non-destructive and requires a small sample volume for measurement.[18] Additionally, DLS has been used to monitor and characterize aggregation in QDs, which could be useful as NPLs, have the potential to aggregate.[19] However, previous studies have not utilized DLS for the characterization and quantification of the lateral size of nanoplatelets.

The overall goal of this study was twofold. First we sought to determine if DLS could be used to determine the lateral size of CdSe NPLs. Second we sought to quantify the molar absorptivity of 3-ML CdSe NPLs, as it has not been reported in the literature. There were four steps required to accomplish these goals. (1) Develop a method of synthesizing pure and stable CdSe NPLs of consistent thickness. (2) Analyze and characterize these NPLs by UV-Visible absorption and fluorescence spectroscopies; to determine the thicknesses. (3) Determine their lateral size by DLS and TEM. The TEM would also support the characterization of the NPLs relative purity by confirming the presence of aggregates. (4) Determine the molar absorptivity using ICP-OES. These values are compared to literature values of 4- and 5-ML NPLs to see if the results are reasonable and provide some confidence in the determined values.

Experimental Methods

Synthesis of Cadmium myristate

Following the procedure established by Dubertret et al, cadmium myristate ($Cd(myr)_2$) was synthesized as an NPL precursor.[16] A solution was made by dissolving cadmium nitrate tetrahydrate, $Cd(NO_3)_2 \cdot 4H_2O$, (0.833 g, 3.52mmol) in 20 mL methanol. A second solution was prepared by dissolving sodium myristate, Na(myr), (1.602 g, 6.40 mmol) in 125 mL of methanol. The solutions were mixed to form cadmium myristate, $Cd(myr)_2$, as a precipitate. The precipitate was vacuum filtered and rinsed three times with methanol. This resulted in a wet, white solid (approximately 3 g, 200% yield), this was not tested for purity and instead was immediately used for the synthesis of CdSe NPLs.

Synthesis of CdSe NPLs

Before syntheses were started, the flasks were thoroughly rinsed with DI water and dried upon removal from the base bath in which they were cleaned, to prevent saponification between the base and the myristate. In the optimized reaction procedure, $Cd(myr)_2$, octadecene (ODE), and Se were combined in a 100 mL four-necked round bottom flask, in the amounts described below in Figure 3A, with a magnetic stir bar. On a N_2 Schlenk line with a thermo-couple controlled heating mantle, the reaction flask was pump-purged three times at 60 ℃, then heated over a period of 20 minutes to 200 °C. When the flask reached 130 °C, solid cadmium acetate, $Cd(Ac)_2$ was added to the reaction flask through one of the flask necks. Upon reaching 200 °C, the NPLs were allowed to grow for select times (1-30 minutes); NPL growth was quenched by pulling aliquots with a syringe through the septa and added into a vial with ODE. The setup for this reaction can be seen below in Figure 3. Nine total runs were completed and the full description of the parameters for each synthesis can be seen in Table S1.

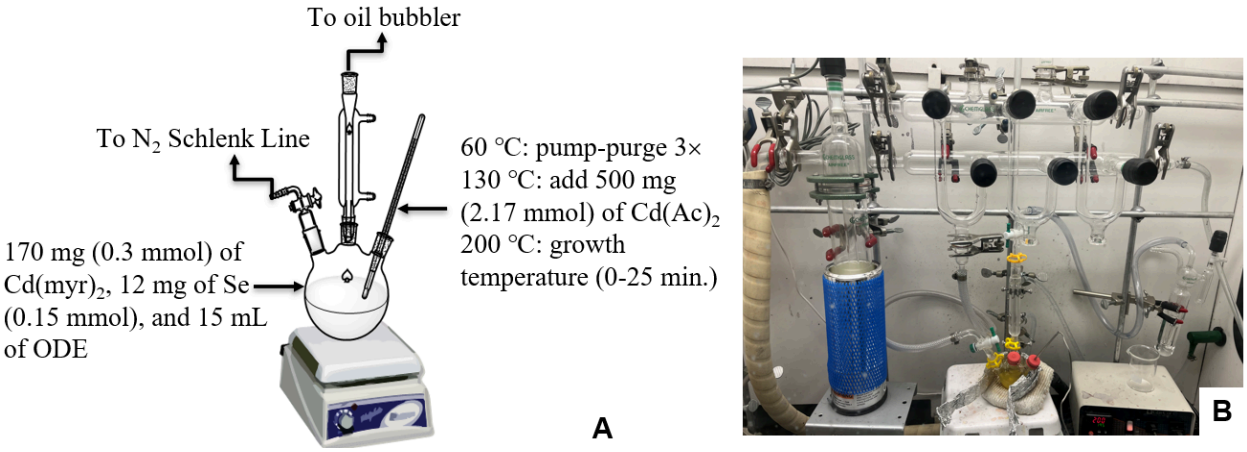

Figure 3. A) Cartoon representation of the experimental setup for the synthesis of CdSe NPLs **B)** Picture of the actual experimental setup for the synthesis of CdSe NPLs.

Purification of CdSe NPLs

CdSe NPLs were typically purified by precipitation with polar solvents and centrifugation. Hexanes, methanol (approximately 5 mL each) and butanol (approximately 3 mL) were added to the CdSe NPL samples in a centrifuge tube. More of each was added (hexanes, methanol and/or butanol) until the layers flocculated. The solutions were centrifuged on an Eppendorf Centrifuge 5702 for 5 minutes at 3600 rpm (2500 g), the supernatant was poured off, and the pellet was kept. The general purification process was repeated three times and the purified NPLs were redissolved in hexanes.

Alternatively, some NPL samples were purified by allowing them to sit overnight and separate out naturally. A ‘soft’ spin (2000 rpm, 1400 g, for 5 minutes) was completed, keeping the supernatants only. Analysis was done only for the supernatants following this size separation.

Analysis and Characterization by UV-Vis and Fluorescence

All UV-Vis analysis was performed on a Varian Cary 50 UV/Vis Spectrophotometer measuring from 300-700 nm. Fluorescence analysis was performed on a PTI Quantumaster 50 through an emission scan run from 420-650 nm using an excitation wavelength of 400 nm and 0.1 s integration. Additional fluorescence analysis was performed through emission scans utilizing an excitation wavelength of 340 nm and running from 370-700 nm.

Analysis and Characterization of Lateral Growth by TEM and DLS

DLS analysis was performed on a Malvern Zetasizer nano-series for synthesis 6 and synthesis 9 samples (see SI Table). TEM analysis was performed on the Transmission Electron Microscope (High Resolution)- JEOL JEM 2010 at the University of Buffalo. Size analysis for synthesis 9 samples was done by hand using ImageJ with the number of analyzed particles between 5-8.

Analysis by ICP-OES

Solutions of synthesis 9 samples 1-4 were prepared for analysis by ICP-OES. The NPLs were "crashed out" by mixing 0.5 mL of reaction solution with approximately 1 mL each of hexanes, methanol, and butanol then centrifuging for 10 minutes at 4000 rpm (2700 g). The supernatant was poured off and the pellets were left to dry for several days at ambient temperature and pressure, to ensure full evaporation of the organic solvents. The NPLs were then digested in 1-2 mL of aqua regia for 3 hours. The solutions were analytically transferred to 25 mL volumetric flasks and brought to volume with 3% HNO_3 in ultrapure water. 5 mL of each solution was placed into centrifuge tubes for unknown concentration measurement. Standards of Cd and Se were purchased, diluted to known concentrations, and prepared for ICP-OES analysis by other members of the Peterson Research Team. The standards were analyzed to create calibration curves. ICP-OES analysis was performed on an iCAP 7000 Series ICP Spectrometer (with Ar flow at 0.5 L/min started 2 hours prior, pump speed at 45-50 rpm and the NESLAB ThermoFlex900 water chiller at 19 ℃) using the program Qtegra.

Results and Discussion

Optimization of Synthesis Procedure

The UV-Vis data for all syntheses revealed that the general synthesis method was capable of synthesizing NPLs as shown by the characteristic double peak, as previously discussed. The first of the double peaks, at approximately 460 nm, was compared to values in the literature and the NPLs were determined to have a thickness of 3-ML.[17] However, some impurities were also observed, as seen by the additional small peaks between 500 and 550 nm in the Synthesis 1 spectra (Figure 4). These impurity peaks were indicative of 4- and 5-ML NPLs. Additionally, although the peaks line up in the UV-Vis, it is clear that there are differences in character as the double peak signal is more distinct in the 10 minute sample than in the 5 minute sample. Therefore, changes were made to optimize the procedure by changing the amount of Cd injected during the secondary addition.

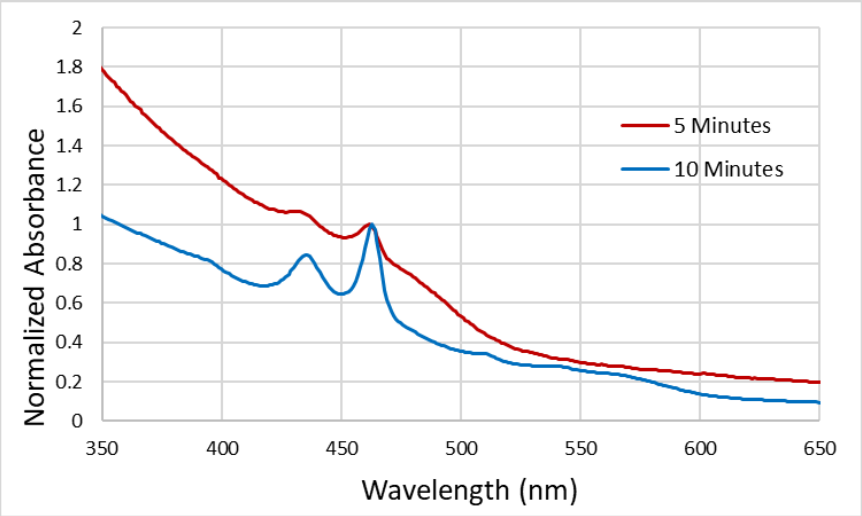

Figure 4. Normalized Data for the absorbance of synthesis 1 products, taken at 5 minutes (1-1) and 10 minutes (1-2) after addition of $Cd(Ac)_2$ and being heated to 200 ℃. The first peaks line up at approximately 460 nm.

Even before the flask reaches 200 ℃ there is some initial growth of 3-ML CdSe NPLs as indicated by the peak at 460 nm (Figure 5). However, the peak grows sharply following the secondary addition of cadmium and it appears that the secondary addition expedites the growth process. Synthesis 8 analyzed the necessity of a secondary addition of Cd, since it is already in excess, and it revealed that increasing the amount of Cd, adding the secondary addition, produced sharper absorption peaks as seen above in Figure 5. As seen in Table S1, changes were made as to the exact amount of this secondary addition in order to optimize the mole ratio and obtain the best results in the UV-Vis.

Investigations into potential changes in sample purity with growth time also revealed a severe problem with stability. Long growth times seemed to decrease stability so much that it was impossible to keep the sample in solution long enough to measure UV-Vis for certain samples and others had extremely low signals or no signal at all. This can be seen in Figure S1 in the supplemental information. The maximum growth time before the sample stability deteriorated seemed to be around 20-25 minutes.

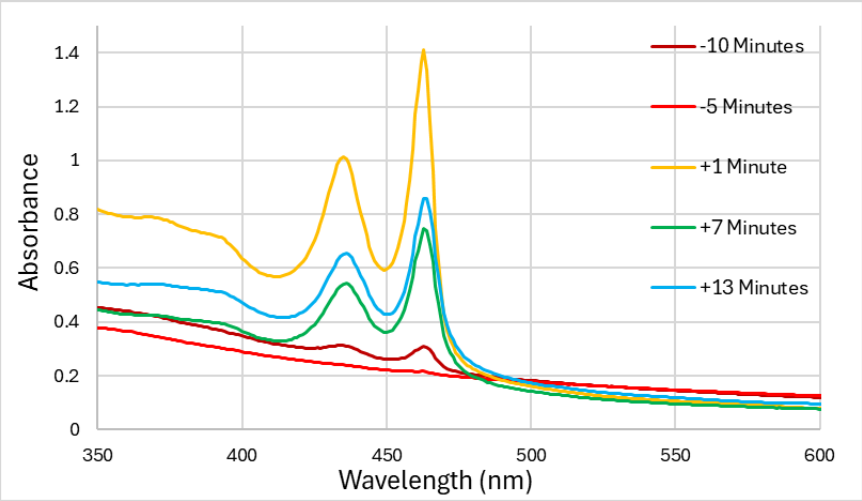

Figure 5. Data for the absorbance of select synthesis 8 products, those taken before (-) and after (+) the secondary addition of cadmium. Peaks line up around 460 nm showing a consistent NPL thickness.

Characterization of Lateral Growth by TEM and DLS

Select results of the TEM analysis are shown below along with the tabulated results and a growth curve showing lateral size as a function of time (Figure 6, Table 1). The TEM provided visual evidence for the success of the reaction and formation of NPLs. Although absorbance suggested formation of NPLs at 0 growth time, the TEM lacked clear NPLs like those shown in the other samples with larger growth times, we suspect they might have something of a seed for the growth of the NPLs. Additionally in several images the NPLs appeared to be rolled, curving or rounded in some spots but straight in others, which complicated analysis more. Several TEM images displayed “wormlike" (curved, dark, and thick lines) structures (highlighted by red box in Figure 6D), which indicate the formation of aggregates.[17] The average diameters for the NPLs are shown in Table 1, along with a predicted value for the 0 minute sample. As the NPLs appeared to be rectangular (Figure 6) the average length and width of a selection of NPLs was measured in ImageJ and the area was calculated from those measurements for the 5, 15, and 25 minute samples. Average effective diameters were calculated by taking the square root of the average areas. These averages were plotted as a function of the square root of time and an effective diameter for the 0 minute sample was backed out from that plot (Figure S7). Interestingly the growth trend appears to be linear (Figure 7) when lateral growth is plotted as a function of time. This does follow the expected trend which is promising for the veritability of this synthesis method.

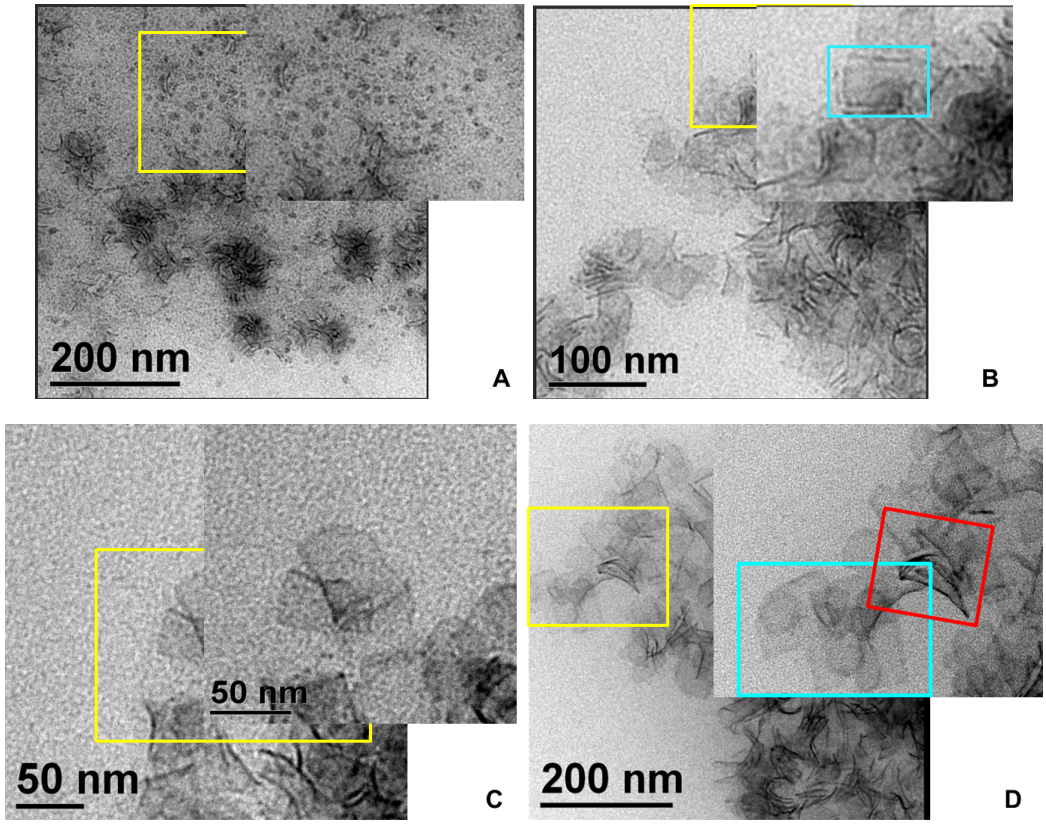

Figure 6. Representative TEM images for synthesis 9 products with growth times of A) 0 minutes (9-1); B) 5 minutes (9-2); C) 15 minutes (9-3) and D) 25 minutes (9-4) after being heated to 200 ℃. Magnification for these images were at 20k× for the 200 nm scale, 12k× for the 100 nm scale and 40k× for the 50 nm scale.

Table 1. Size Determination and Comparison of Synthesis 9 Products by TEM and DLS Analyses

Growth Time at 200 ℃	TEM Size Determination	DLS Size Determination
0 Minutes (calculated)	28 (5) nm (calculated)	1112 (186) nm
5 Minutes (N=5)	39 (3) nm	2157 (1040) nm
15 Minutes (N=7)	50(3) nm	1874 (581) nm
25 Minutes (N=8)	62 (4) nm	2641 (574) nm

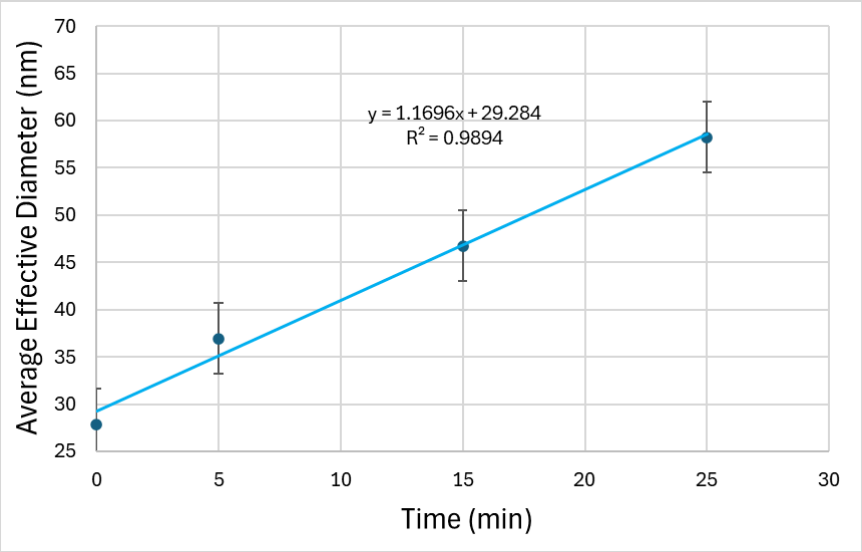

Figure 7. Growth rate for synthesis 9 nanoplatelets as analyzed by TEM where the average effective diameter is represented as a function of time.

The lateral size of the same samples measured by TEM was also characterized by DLS. There was some trend of the size increasing as time increased (Figure 8); however, the sizes were much larger than expected from the TEM analysis. This could be due to aggregation or contamination by large particles, but further testing would still be required. As TEM is the established method, it does seem to indicate that the DLS is an unreliable method given the DLS numbers are much larger than those for the TEM. However, it is possible that changes could be made to the procedure preceding DLS analysis that could improve the results. Some examples could be sonicating the samples to try and break up aggregates and/or filtering them to try and remove large particles (aggregates or contaminants).

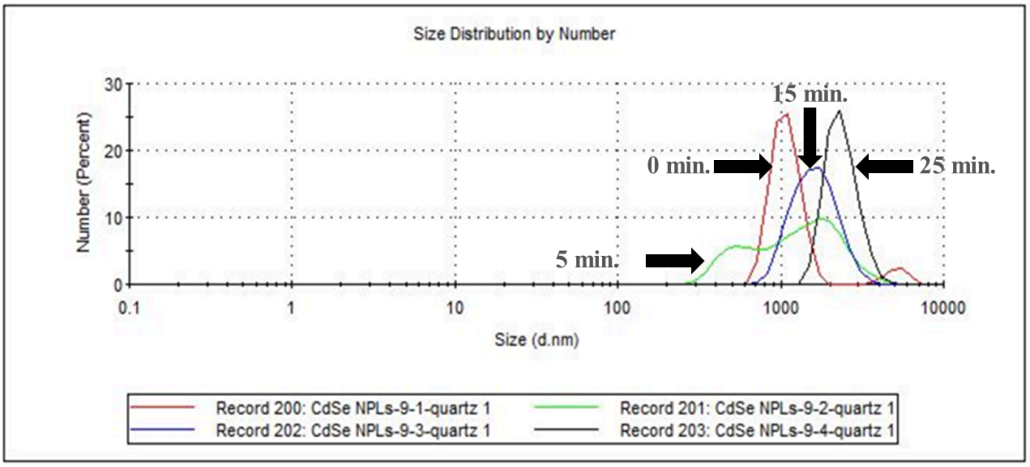

Figure 8. DLS analysis of synthesis 9 products, taken at 0 minutes (9-1), 5 minutes (9-2), 15 minutes (9-3), and 25 minutes (9-4) after reaching the growth temperature of 200 ℃ with products in a quartz cuvette and ODE as the solvent.

Characterization of Optical Properties

Characteristic examples of typical UV-Vis and fluorescence spectra from two different synthetic runs are shown in Figure 9 A and B. The peaks from both samples of both syntheses appear almost identical in peak wavelength and shape are indicative of consistency in the synthesis method. The fluorescence data is also consistent with what is expected according to the literature, with the fluorescence peak being shifted just to the red of the first peak in the UV-Vis double peaks, 464.2 nm compared to the 464 nm of the absorbance. However, there were also some areas of concern in the fluorescence data that required additional analysis. There were large, broad signals starting around 630 nm, as well as small peaks around 515 nm, which are especially visible in Figure 9 A. The smaller peaks are most likely 4-ML NPLs, as that is their characteristic peak.[13] The lack of their presence in UV-Vis could be due to them being in low concentration and so are not visible compared to the large peaks for the 3-ML NPLs. As for the broad emission signals, a second fluorescence measurement was performed using a lower energy excitation wavelength of 500 nm (Figure 10).

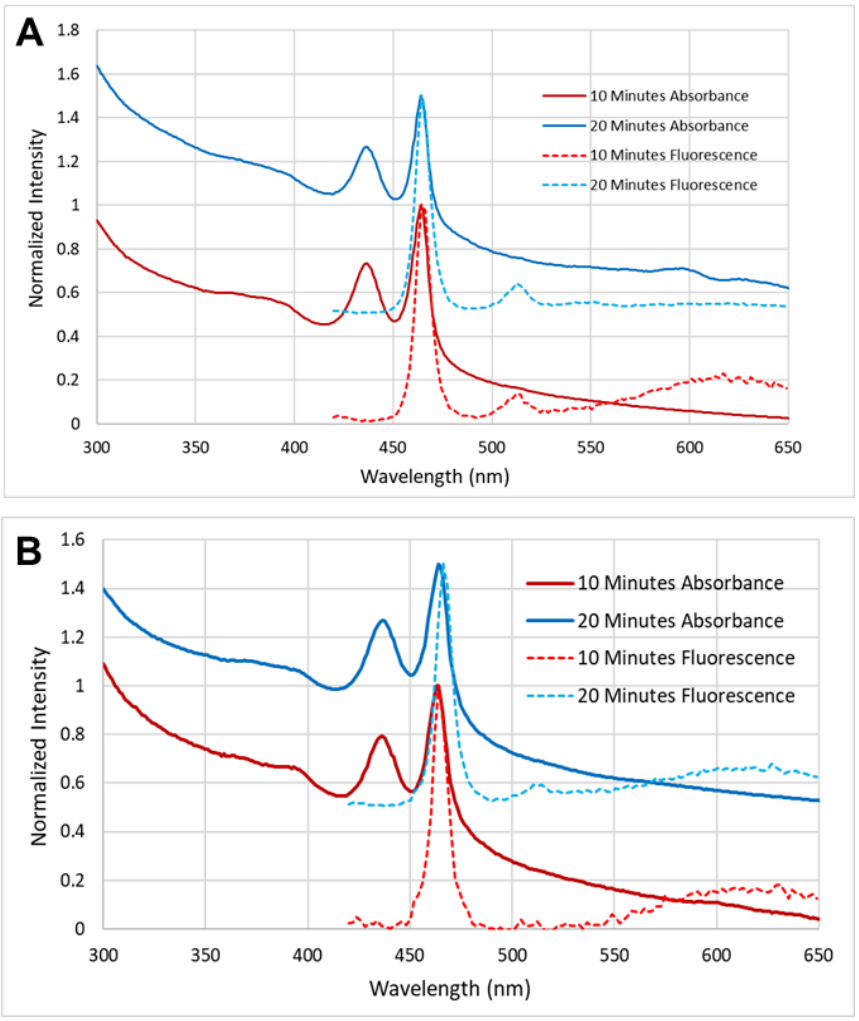

Figure 9. A) Normalized and stacked data for the fluorescence (400 nm excitation) and absorbance of synthesis 3 products, taken at 10 minutes (3-1) and 20 minutes (3-2) after addition of $Cd(Ac)_2$ and being heated to 200 ℃. **B)** Normalized and stacked data for the fluorescence (400 nm excitation) and absorbance of synthesis 4 products, taken at 10 minutes (4-1) and 20 minutes (4-2) after addition of $Cd(Ac)_2$ and being heated to 200 ℃. In both 9 (a) and 9 (b) peaks line up around 460 nm showing a consistent NPL thickness.

A second scan was done to determine if there was an additional NP that was causing the large, broad emission or something else. The lower energy scan revealed that there was not a secondary particle causing the emissions past 520 nm, rather it was associated with the intensity at 460 nm, likely due to trap emission. This trap emission could have been deep-level traps, such as vacancies in the surface, which would be why they would have required higher energy to emit and disappeared with the lower energy excitation.[20,21, 22]

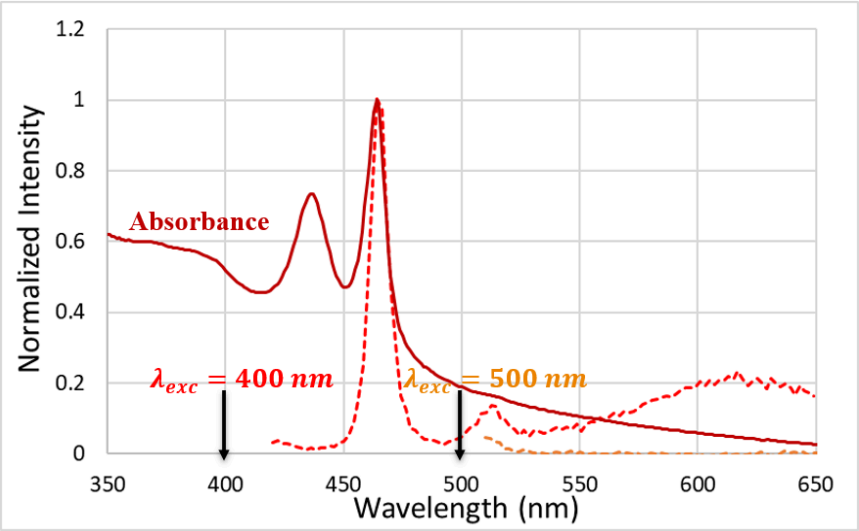

Figure 10. Isolated graph of the synthesis 3 product with 10 minute growth time (3-1). Reveals the emission at ~460 nm and shows that trap emission created extra signal that does not correspond to any further NPs.

Characterization of molar absorptivity by ICP OES

The absorbance data from Figure 11 A was used for the determination of the molar absorptivity values. Figure 11 B shows the normalized absorption peaks, which makes it easier for a direct comparison of the four samples at their respective peaks. What made this data interesting is that the curve for the 25 minute growth time sample there is a bathochromic shift when compared to the other three curves at earlier times. This supports the observation that after 20 minutes of growth time there seem to be some oddities in the properties and stability of the NPLs. Additionally, the 5 minute sample appeared to have more impurities as seen by the sharp rise after 400 nm, which was higher than those of the other three samples.

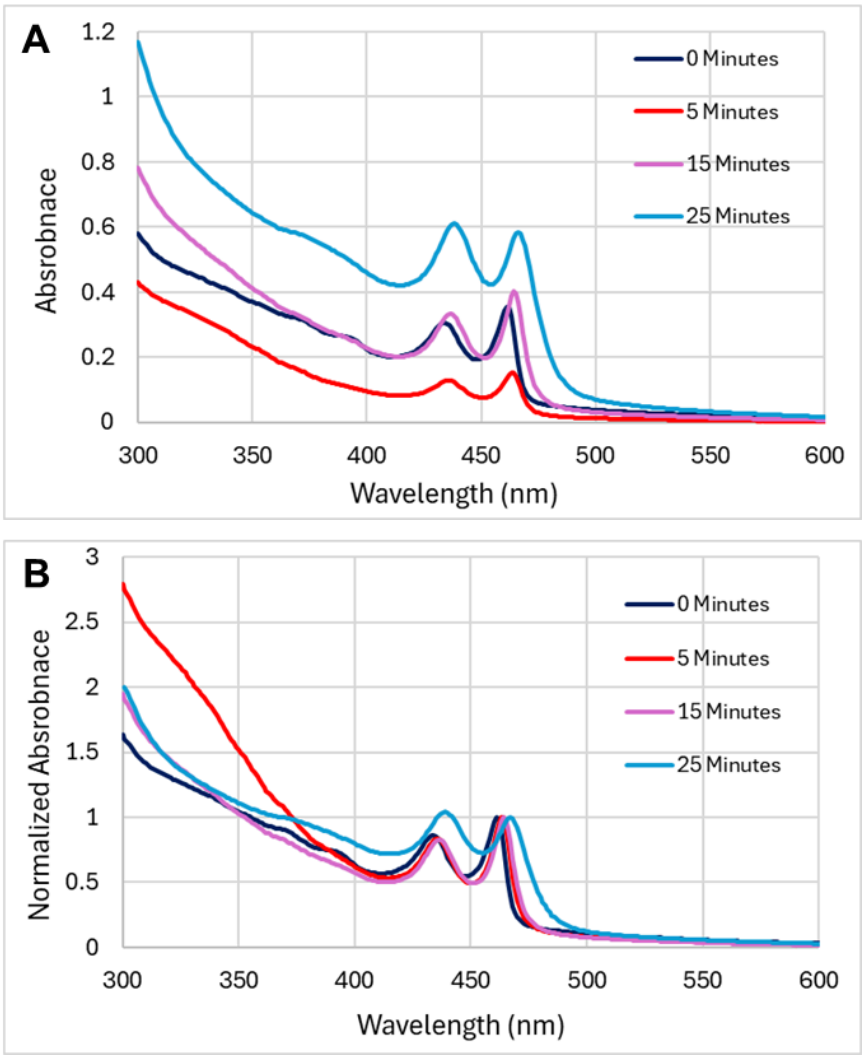

Figure 11. A) data for the absorbance of synthesis 9 products, taken at 0 minutes (9-1); 5 minutes (9-2); 15 minutes (9-3) and 25 minutes (9-4) after being heated to 200 ℃. **B)** Normalized data for the absorbance of synthesis 9 products, taken at 0 minutes (9-1); 5 minutes (9-2); 15 minutes (9-3) and 25 minutes (9-4) after being heated to 200 ℃. Samples measured in a microcuvette with a pathlength of 4 mm.

Calibration curves were created for both Cd and Se using known standards (Figure 12). From these curves the concentration of Cd and Se were determined for each of the unknown NPL samples, along with their error (Table 2). These concentrations, along with reported material parameters,[23] were then used to calculate the concentration of the NPLs in each sample using equation 1, and reported in Table 2.

$$Concentration\ of\ NPLs\ (M) = \left(\frac{Concentration\ of\ Se\ (ppb)}{Molar\ Mass\ of\ Se} \times 10^{-6}\right)\left(\frac{Molar\ Mass\ of\ CdSe}{V_{NP} d N_A}\right) \quad \textbf{(1)}$$

As can be seen in Table 2, the stoichiometric ratio of Cd:Se is not 1:1 as it should have been, given the formula is simply CdSe. The Cd was found to be in much higher concentrations compared to the Se, especially for the samples at shorter growth times. A possible explanation for this is the use of excess Cd in the synthesis method. The original reaction mixture is in a 2:1 Cd:Se molar ratio, then upon the secondary addition that ratio changes to almost 16.5:1. This Cd rich environment could even be producing Cd terminating surfaces. Further ICP-OES analysis would be useful to look into this phenomenon.

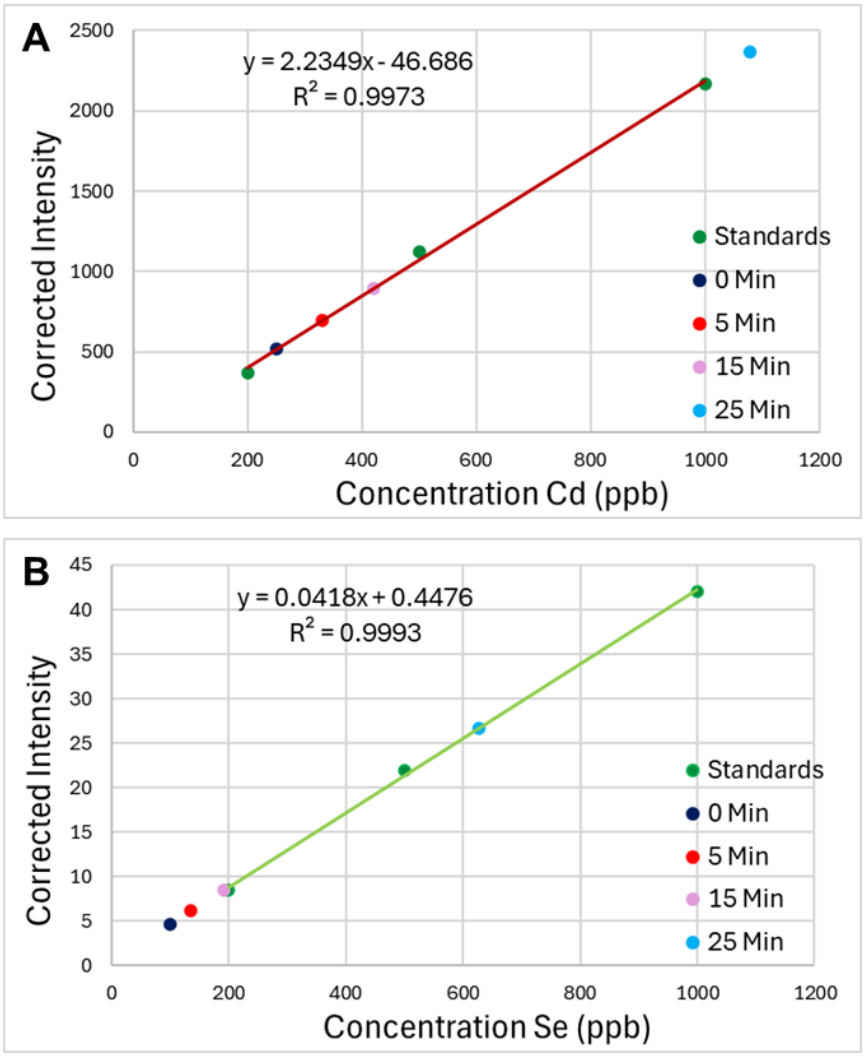

Figure 12. Calibration curves for the determination of the concentration of **A)** Cd and **B)** Se in synthesis 9 products using standards at 3 known concentrations for each.

Table 2. Cd, Se, and NPL Concentrations for Synthesis 9 Products from ICP-OES Analysis

Growth Time at 200 ℃	Cd Concentration (M)	Se Concentration (M)	NPL Concentration (M)
0 Minutes	$1.12\ (0.16) \times 10^{-4}$	$6.40\ (0.11) \times 10^{-5}$	$4.30\ (0.41) \times 10^{-9}$
5 Minutes	$1.47\ (0.17) \times 10^{-4}$	$8.60\ (0.11) \times 10^{-5}$	$3.30\ (0.44) \times 10^{-9}$
15 Minutes	$1.88\ (0.18) \times 10^{-4}$	$1.21\ (0.12) \times 10^{-4}$	$2.89\ (0.29) \times 10^{-9}$
25 Minutes	$4.80\ (0.29) \times 10^{-4}$	$3.97\ (0.16) \times 10^{-4}$	$6.11\ (0.26) \times 10^{-9}$

Using this final concentration and values for the absorbance, at both the maximum absorbance (at approximately 460 nm) and at high energy (350 nm) Beer's Law was utilized to calculate the molar absorptivity (Table 3).

Table 3. Molar Absorptivities for Synthesis 9 Products from ICP-OES, UV-Vis and TEM Analyses

Growth Time at 200 ℃	Molar Absorptivity at 460 nm ($M^{-1}cm^{-1}$)	Molar Absorptivity at 350 nm ($M^{-1}cm^{-1}$)
0 Minutes	$2.07\ (0.20) \times 10^{8}$	$2.15\ (0.20) \times 10^{8}$
5 Minutes	$1.16\ (0.16) \times 10^{8}$	$1.77\ (0.24) \times 10^{8}$
15 Minutes	$3.47\ (0.35) \times 10^{8}$	$3.57\ (0.36) \times 10^{8}$
25 Minutes	$2.39\ (0.10) \times 10^{8}$	$2.64\ (0.11) \times 10^{8}$

In comparison to literature values for 4- and 5-ML CdSe NPLs, the 3-ML NPL molar absorptivities are more similar to those of the 5-ML, at least in terms of relative magnitude.[13] Critically, however, this could be due to the large lateral size of the 3-ML NPLs compared to 4-ML (with sizes ranging from approximately 30-60 nm vs sizes ranging from approximately 10-20 nm, respectively)[13], as there is a direct relationship between the lateral size of the NPL and its molar absorptivity. To account for the lateral size dependence, the absorption coefficient (α) was determined (equation 2), as has been reported for other shapes of CdSe NPs.[15,24] The currently reported absorption coefficients, as well as values derived from other literature reports for 4- and 5-ML CdSe NPLs, are shown in Figure 14.

$$\alpha = \frac{2303\varepsilon}{N_A V_{NP}} \quad \textbf{(2)}$$

In previous studies of CdSe QDs, the absorption coefficient at energies greater than 3 eV was constant, i.e. an α of 1.3×10^5 cm^{-1} at 3.54 eV, regardless of QD size.[15] However, that specific value was not observed in the NPL sample, in neither the two samples from previous literature (from which α was extrapolated for use in this comparison)[13] nor the current experimentally measured value. The absorption coefficients for the synthesis 9 samples are listed below in Table 4 both at the peak energy, around 2.7 eV, and at 3.54 eV. All of these values are much larger than that for QDs, and they are not constant at neither the peak energy nor high energy even amongst each other. Those inconsistencies can also be seen in Figure 13. As volume is accounted for in the calculation for absorption coefficient, a possible explanation for the disparities in values is the differences in concentrations. As mentioned, the concentrations were not what they were expected to be and that could be causing issues with the other values that depend on them for their calculations, like molar absorptivity and absorption coefficient. Despite these inconsistencies, there was at least one consistent trend observed amongst NPLs of different thicknesses. This trend saw that peak absorption coefficient increased as the number of monolayers decreased (Figure 14). The relatively similar appearance of each of the curves along with the 3-ML NPL following the trend set by the literature values provides some confidence as to the success of the synthesis and analysis of the NPLs, even if the magnitude of the values are larger than expected.

Table 4. Absorption Coefficients for Synthesis 9 Products

Growth Time at 200 ℃	Absorption Coefficient at 2.7 eV	Absorption Coefficient at 3.54 eV
0 Minutes	$9.7\ (8.2) \times 10^5$	$1.01\ (0.86) \times 10^6$
5 Minutes	$5.4\ (1.0) \times 10^5$	$8.3\ (1.6) \times 10^5$
15 Minutes	$1.63\ (0.24) \times 10^6$	$1.67\ (0.24) \times 10^6$
25 Minutes	$1.12\ (0.09) \times 10^6$	$1.24\ (0.10) \times 10^6$
Average	$\mathbf{1.07\ (0.22) \times 10^6}$	$\mathbf{1.19\ (0.18) \times 10^6}$

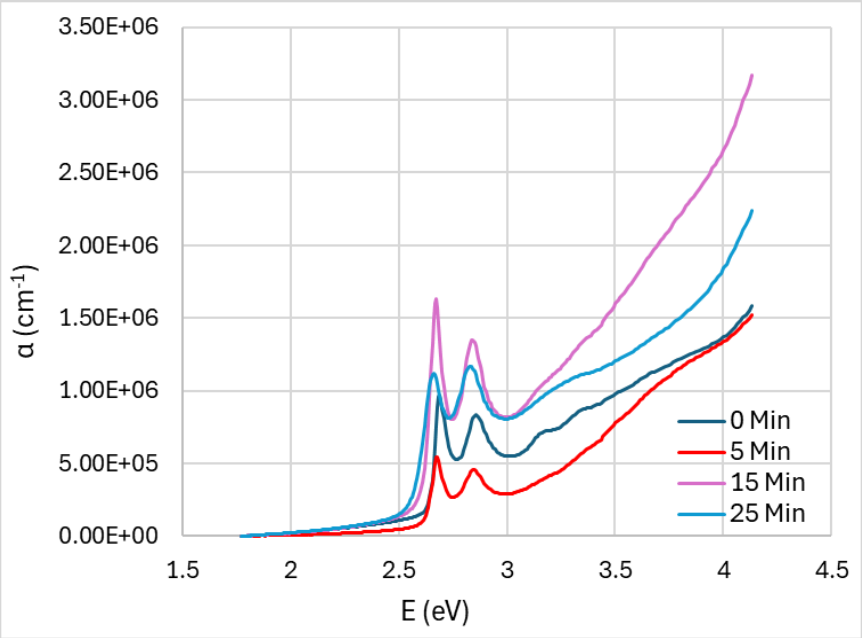

Figure 13. Plot of absorption coefficient (α) as a function of energy for synthesis 9 products, taken at 0 minutes (9-1); 5 minutes (9-2); 15 minutes (9-3) and 25 minutes (9-4) after being heated to 200 ℃.

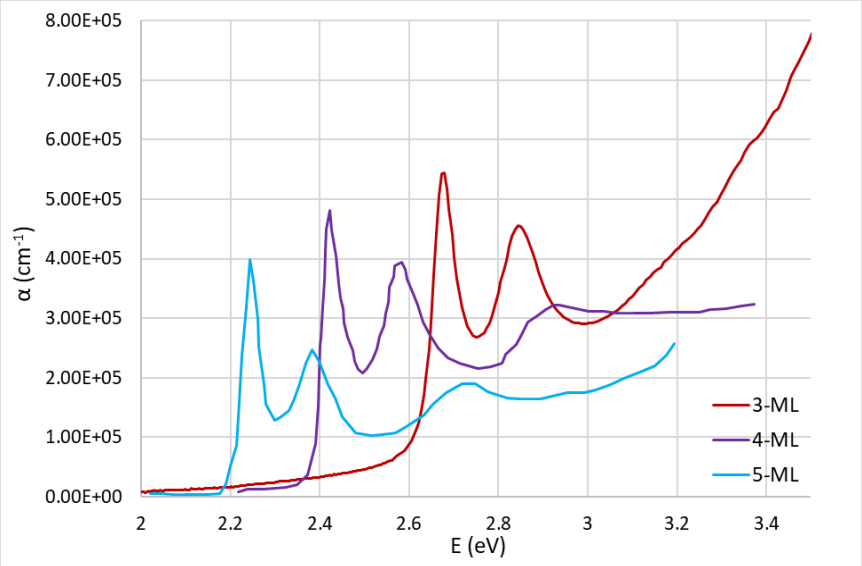

Figure 14. Plot of absorption coefficient (α) as a function of energy for the comparison of experimental (3-ML) NPLs with known values for 4- and 5-ML NPLs.[13]

Conclusion

The molar absorptivity (ε) has been measured for 3-ML CdSe NPLs for the first time. The molar absorptivity was found to be on the order of 10^8 $M^{-1}cm^{-1}$ depending on lateral size. However, as 3-ML NPLs have not been researched thoroughly, an important next step would be to synthesize NPLs of larger thicknesses (4- ML and/or 5- ML) in order to validate the method of lateral size and molar absorptivity determinations. Furthermore, it would be helpful to run additional ICP-OES testing to create a larger sample size for NPLs of the same thickness and growth times in order to find an average in case of machine error. Using more standards to create a wider range of known concentrations and calibration curves with more than 3 points could also be helpful to improve the ICP-OES results.

Results from TEM, the confirmed method for measuring the lateral growth of NPLs, appeared to invalidate any results from DLS. This is disappointing because if the TEM and DLS results had been consistent, then DLS could be established as a viable new way to measure lateral growth in NPLs. The discovery of a faster technique for determining lateral growth size, DLS, would be valuable for the enhancement of this field of NPL research. Further testing could still be required before discounting DLS completely as a viable method. Some improvements could be made to the methodology prior to DLS being run. One method could be done after synthesis and that is to use oleic acid for ligand capping to help prevent aggregation.[25] Other ways to improve could be done right before DLS is run is sonicating the samples (possibly breaking up aggregates), using syringe filters to remove any large particles that could be impacting the measurements, and cleaning the cuvettes in a mild acid bath to remove contaminants. Additionally, further testing would be helpful for the analysis of the formation of aggregates. Running TEM, and DLS for additional comparison, at different time periods (right after synthesis and then at various time intervals afterwards) would allow for the determination of aggregate formation.

Acknowledgements

This project would not have been possible without the help of the Geneseo Chemistry Department and especially not without my research advisor Dr. Peterson. Thanks are also necessary to Dr. Webb without whom TEM analysis would not have been possible and Dr. Charlebois for his help in fixing and running the ICP-OES. Additionally, acknowledgements are owed to Amber Wright and Mason Seipel for their help with the completion of this project, along with Emily Rennells and Timothy Atkins for their work in creating standards for and calibrating the ICP-OES for the analysis of unknown samples.

References

1. *Colloidal Quantum Dot Optoelectronics and Photovoltaics*, 1st ed.; Konstantatos, G., Sargent, E. H., Eds.; Cambridge University Press, **2013**. DOI: 10.1017/CBO9781139022750
2. Efros, A. L.; Brus, L. E. Nanocrystal Quantum Dots: From Discovery to Modern Development. *ACS Nano.* **2021**, *15* (4), 6192-6210.
3. Malik, S.; Muhammad, K.; Waheed, Y. Emerging Applications of Nanotechnology in Healthcare and Medicine. *Molecules* **2023**, *28* (18), 6624.
4. Khan, I.; Saeed, K.; Khan, I. Nanoparticles: Properties, applications and toxicities. *Arab. J. Chem.* **2019**, *12* (7), 908-931.
5. Bailey, R.; Smith, A.; Nie, S. Quantum dots in biology and medicine. *Physica E Low Dimens. Syst. Nanostruct.* **2004**, *25* (1), 1-12.
6. Raffaelle, R. P.; Castro, S. L.; Hepp, A. F.; Bailey, S. G. *Prog. Photovolt.* **2002**, *10*, 433-439.
7. Coe, S.; Woo,W. K.; Bawendi, M. G.; Bulovic, V. Electroluminescence from single monolayers of nanocrystals in molecular organic devices. *Nature.* **2002**, *420*, 800-803.
8. Klimov, V. I.; Mikhailovsky, A. A.; Xu, S.; Malko, A.; Hollingsworth, J. A.; Leatherdale, C. A.; Eisler, H. J.; Bawendi, M. G. Optical gain and stimulated emission in nanocrystal quantum dots. *Science.* **2000**, *290* (5490), 314-317.
9. Bruchez, Jr. M.; Moronne, M.; Gin, P.; Weiss, S.; Alivisatos, A. P. Semiconductor nanocrystals as fluorescent biological labels. *Science.* **1998**, *281* (5385), 2013-2016.
10. Payal, P. Role of Nanotechnology in Electronics: A Review of Recent Developments and Patents. *Recent Pat. Nanotechnol.* **2022**, *16* (1), 45-66.
11. Joo J.; Son J. S.; Kwon S. G.; Yu J. H.; Hyeon T. Low-temperature solution-phase synthesis of quantum well structured CdSe nanoribbons. *J. Am. Chem. Soc.* **2006**, *128*, 5632–5633.
12. Ithurria S.; Dubertret B. Quasi 2D colloidal CdSe platelets with thicknesses controlled at the atomic level. *J. Am. Chem. Soc.* 2008, 130, 16504–16505.
13. Yeltik, A.; Delikanli, S.; Olutas, M.; Kelestemur, Y.; Guzelturk, B.; Demir, H. V. Experimental Determination of the Absorption Cross-Section and Molar Extinction Coefficient of Colloidal CdSe Nanoplatelets. *J. Phys. Chem. C.* **2015**, *119* (47), 26768–26775.
14. Yu, W. W.; Qu, L.; Guo, W.; Peng, X. Experimental Determination of the Extinction Coefficient of CdTe, CdSe, and Cds Nanocrystals. *Chem. Mater.* **2003**, *15* (14), 2854–2860.
15. Jasieniak, J.; Smith, L.; van Embden, J.; Mulvaney, P.; Califano, M. Re-examination of the Size-Dependent Absorption Properties of CdSe Quantum Dots. *J. Phys. Chem. C.* **2009**, *113* (45), 19468–19474.

16. Ithurria, S.; Bousquet, G.; Dubertret, B. Continuous Transition from 3D to 1d Confinement Observed during the Formation of CdSe Nanoplatelets. *J. Am. Chem. Soc.* **2011**, *133* (9), 3070–3077.
17. Jiang, Y.; Ojo, W.; Mahler, B.; Xu, X.; Abécassis, B.; Dubertret, B. Synthesis of CdSe Nanoplatelets without Short-Chain Ligands: Implication for Their Growth Mechanisms. *ACS Omega* **2018**, *3* (6), 6199-6205.
18. Wyatt Technology, Waters Corporation. https://www.wyatt.com/solutions/techniques/dynamic-light-scattering-nanoparticle-size.html (Accessed April 16, 2024)
19. Rodriguez-Loya, J.; Lerma, M.; Gardea-Torresdey, J. L. Dynamic Light Scattering and Its Application to Control Nanoparticle Aggregation in Colloidal Systems: A Review. *Micromachines (Basel)* **2024**, *15* (1), 24.
20. Baker, D. R.; Kamat, P. V. Tuning the Emission of CdSe Quantum Dots by Controlled Trap Enhancement. *Langmuir* **2010**, *26* (13), 11272-11276.
21. Veamatahau, A.; Jiang, B.; Seifert, T.; Makuta, S.; Latham, K.; Kanehara, M.; Teranishi, T.; Tachibana, Y. Origin of surface trap states in CdS quantum dots: relationship between size dependent photoluminescence and sulfur vacancy trap states *Phys. Chem. Chem. Phys.*, **2015**, *17*, 2850-2858
22. Hinterding, S. O. M.; Salzmann, B. B. V.; Vonk, S. J. W.; Vanmaekelbergh, D.; Weckhuysen, B. M. Single Trap States in Single CdSe Nanoplatelets. *ACS Nano*. **2021**, *15* (4), 7216-7225.
23. Madelung, O. *Semiconductors Data Handbook*; Springer-Verlag Berlin Heidelberg, **2004**.
24. Shaviv, E.; Salant, A.; Banin, U. Size Dependence of Molar Absorption Coefficients of CdSe Semiconductor Quantum Rods. *Chem. Phys. Chem.* **2009**, *10* (7), 1028-1031.
25. Wang, X.; Hao, J.; Cheng, J.; Li, J. Chiral CdSe nanoplatelets as an ultrasensitive probe for lead ion sensing. *Nanoscale*. **2019**, *11*(19), 9327-9334.